Implementing internal interfaces in finite-difference schemes with the Heaviside step function

Rune Mittet, EMGS

SUMMARY

Implementing sharp internal interfaces in finite-difference schemes with high spatial accuracy is challenging. The implementations of interfaces are generally considered accurate to at best second order. The natural way to describe an abrupt change in material parameters is by the use of the Heaviside step function. However, the implementation of the Heaviside step function must be consistent with the discrete sampling on the finite-difference grid. Assuming that the step function takes on the value zero up to some node location and then unity from thereon results in an incorrect wavenumber representation of the Heaviside step function so this representation must be incorrect. However, starting with the proper wavenumber representation of the Heaviside step function and then transforming this spectrum to the space domain give much better accuracy. The interface location appears as a proportionality factor in the phase in the wavenumber domain and can be altered continuously. Thus, the interface can be located anywhere between two node locations. This is a key factor for avoiding stair-case effects from the fields when doing 2D and 3D finite-difference simulations. The proposed method can be used for all systems of partial differential equations that formally can be expressed as a material parameter times a dynamic field on one side of the equal sign and with spatial derivatives on the other side of the equal sign. For geophysical simulations the most important cases will be the Maxwell equations and the acoustic and elastic wave equations.

INTRODUCTION

Despite extensive developments of high-order finite-difference schemes over the last four decades, the method is only first order accurate when it comes to simulating sharp internal material-parameter discontinuities, if no medium averaging techniques are used (Gustaffson and Wahlund, 2004; Symes and Vdovina, 2009). Alternatively, the finite difference method can be considered second order accurate with respect to implementation of interfaces if parameter averaging of the type proposed by Moczo et al. (2002) is used (Vishnevsky et al., 2014). The low order accuracy favors grids with short spatial steplengths relative to typical wavelengths. On the other hand, both the CPU time and the memory size required to simulate a 3D problem with finite differences are drastically reduced with large steplengths. One problem with increasing the steplength is the potential increase in the spatial dispersion error. This problem can be mitigated by using a pseudo-spectral implementation for the numerical differentiation or the spatial dispersion error can be kept small in a controlled manner by the application of high-order finite-difference operators. Pseudo-spectral and high-order finite-difference methods can, given that high accuracy at late times is mandatory, propagate fields on grids that are 10 to 20 times coarser than those required for second order

spatial schemes. The problem is obvious if the implementation of internal interfaces is only second order accurate: These high-order methods cannot be fully utilized since the error related to interface locations increases to an unacceptable level.

One attractive property of explicit finite differences is the ease of implementation. Surely, complications increase when external boundaries are implemented in order to simulate a free surface or absorbing boundary conditions at the sidewalls of the computational domain, still, the implementation effort is low compared to many other simulation schemes. Likewise, explicit finite differences are numerically very efficient when properly implemented and serve as the simulation engine in numerous reverse time migration and inversion schemes. The simulation engine must have a low and predictable numerical error. Typical propagation errors such as spatial and temporal dispersion are well understood and can be reduced to a desired or tolerable minimum by high-order methods. Application of high-order methods to reduce temporal dispersion is discussed by Dablain (1986), Tal-Ezer (1986) and Etgen (1989). Alternatively, a post modeling temporal dispersion correction can be performed (Stork, 2013; Anderson et al., 2015).

The interface problem is not too severe in many real data processing cases since for example the seismic migration velocity model is smooth or the seismic velocity or the electromagnetic conductivity model retrieved by inversion is smooth due to limited resolution. However, there may be cases where an accurate description of a sharp interface is required. One example can be the seabed. The location of this interface is often known with higher accuracy than formation interfaces since it can be measured by echo sounding. It is also a high impedance contrast. This is particularly the case for marine CSEM surveys. For both electromagnetic and seismic simulations it might be that accurate simulation results for sediment-salt boundaries are required. These boundaries are strong reflectors and cannot be well described unless a sharp transition is implemented with sufficient accuracy. Here I propose a methodology to simulate sharp internal material-parameter discontinuities at arbitrary positions and discuss some of the limitations with this approach.

THEORY

The problem of properly implementing sharp internal material-parameter discontinuities is present even for very simple finite-difference modeling schemes like the 1D acoustic wave equation. The acoustic wave propagation problem is determined by Newton's second law and the constitutive relation,

$$
\begin{aligned}
\rho(z)\partial_t v_z(z,t) &= \partial_z \sigma(z,t) + \delta(z-z_s)f_z(t), \\
\kappa(z)\partial_t \sigma(z,t) &= \partial_z v_z(z,t).
\end{aligned} \tag{1}
$$

Here ρ is density, v_z is particle velocity in the z-direction, σ is stress, δ is a Dirac delta distribution, f_z is the time function for a force density in the z-direction and κ is compliance.

In finite differences an interface is implemented as a jump in a material parameter. A jump can be described by means of the Heaviside step function. Let us give the upper halfspace index 1 and the lower halfspace index 2. Let the Heaviside step function be denoted $H(z)$ with

$$
\begin{aligned}
H(0^-) &= 0, \\
H(0) &= \tfrac{1}{2}, \\
H(0^+) &= 1, \quad\quad (2)
\end{aligned}
$$

given infinite spatial bandwidth. A sharp interface in compliance is then described by,

$$
\begin{aligned}
\kappa(z) &= \kappa_1 + H(z - z_b)\Delta\kappa, \\
\Delta\kappa &= \kappa_2 - \kappa_1. \quad\quad (3)
\end{aligned}
$$

Step functions must necessarily be bandlimited on a grid with

a finite steplength. Initially, let us assume that the interface location is midway between two nodes. The most intuitive

implementation is as follows: Let the stepfunction equal zero down to a node just above the interface and unity from the node just below the interface. The Fourier amplitude spectrum of the stepfunction described above can be found by performing a discrete Fourier transform of a function that in this example is 0 from node 1 to node 250 and 1 from node 251 to node 1000. The node distance is $\Delta z = 10$ m. The amplitude spectrum as a function of wavenumber is shown with black squares in Figure 1a. On the other hand, we may calculate the frequency spectrum of a bandlimited step function, $\tilde{H}(z - z_b)$, analytically,

$$
\tilde{H}(k_z) = \frac{1}{\Delta z}\frac{2}{k_z}\sin(\tfrac{1}{2}k_z(z_m - z_b))e^{-ik_z\frac{1}{2}(z_m + z_b)}, \quad\quad (4)
$$

and then include only wavenumbers with absolute value less or equal to the spatial Nyquist wavenumber, $k_z^N = \frac{\pi}{\Delta z}$, in the transform from wavenumber domain to space domain. The variable z_b is the interface location and the variable $z_m = (N_z - \frac{1}{2})\Delta z$ with N_z the number of nodes. The analytical amplitude spectrum is plotted with green squares in Figure 1a. It is different from the spectrum of the function of the intuitive implementation. The corresponding space domain functions are shown in Figure 1b. The black curve is just a jump in value from node 250 to node 251. The green curve is the space domain representation of equation 4. This curve shows Gibbs oscillations for nodes 247 to 254. The transition between the upper and lower medium is slightly softer than the intuitive implementation.

Note from equation 4 that the interface location z_b can be moved continuously on the finite-difference grid. No medium averaging is necessary with this implementation of the interface and it can be demonstrated that the accuracy with this implementation is much higher than with averaging techniques (Mittet, 2017).

If the compliance is given by equation 3 then we see that we have a discontinuity on the left-hand side of the second equation 1. This discontinuity must have a counterpart on the right-hand side. Thus, the particle velocity is continuous but has a kink at the interface location such that the derivative of the field makes a jump. The location of the kink in the particle velocity field is at z_b and represents the reflection point (Mittet, 2017).

RESULTS

Several tests for vertically traveling plane waves has been performed in a halfspace model to compare the step function implementation of the interface with an implementation using harmonic averaging of the bulk modulus and arithmetic averaging of the density. The step-function implementation is used for compliance and density which both appear in the left-hand side of equation 1. The source and receiver are at depth 2000 m. The spatial steplength is 10 m. The maximum frequency of the propagating waveform is 50 Hz with the peak frequency at 20 Hz. The jump in density from the top to the bottom layer is from 2000 kg/m^3 to 4000 kg/m^3. The jump in compliance is such that the velocity jumps from 2000 m/s in the upper layer
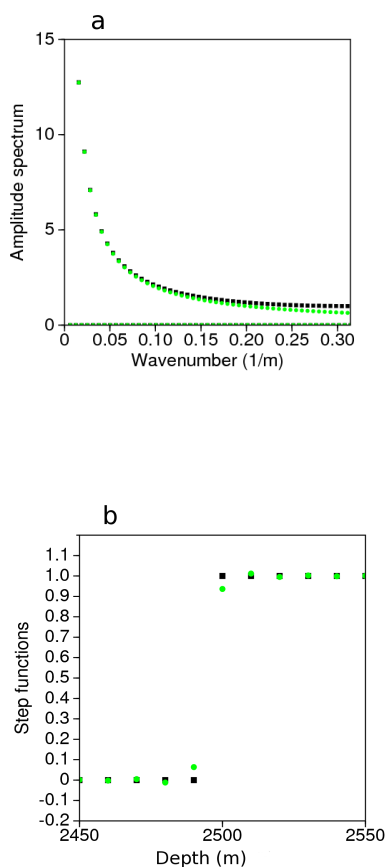
Figure 1: Two representations of the step function. The black curve is a transition from zero to unity from one node to the next. The green curve is a representation of the stepfunction where the transition from zero to unity is properly bandlimited. a) Wavenumber spectrum b) Space domain representation. The Gibbs phenomenon is visible for the green curve.
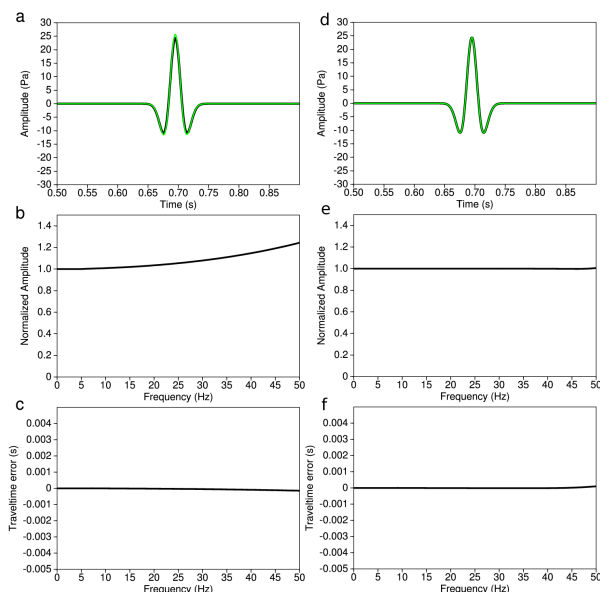
Figure 2: Left column - averaging and right column - step function, interface at 2495 m. a) and d) Analytical - black and FD - green. b) and e) Amplitude ratio. c) and f) Time advance or delay.
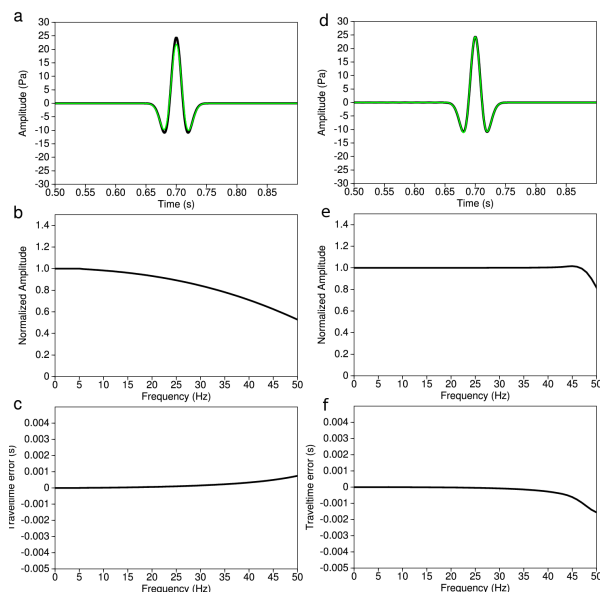

Figure 3: Left column - averaging and right column - step function, interface at 2500 m. a) and d) Analytical - black and FD - green. b) and e) Amplitude ratio. c) and f) Time advance or delay.

to 4000 m/s in the lower layer. Errors are calculated by Fourier transforming the finite-difference (FD) time domain solution and the analytical solution for the problem. The complex FD spectrum is divided by the complex spectrum for the analytical solution. The modulus of this ratio reveals amplitude errors if it deviates from unity. The argument (phase) of this ratio is divided by the angular frequency and reveals traveltime errors if it deviates from zero.

In the first example the interface is at 2495 m. In this case it is midway between nodes. The left column in Figure 2 show the results of using harmonic averaging based on relative volumetric contribution for the bulk modulus and arithmetic averaging of the density also based on relative volumetric contribution. Note that since the interface is midway between nodes the medium changes abruptly from the node at 2490 m to the node at 2500 m. The transition is similar to the black curve in Figure 1. The type of error introduced is mainly in terms of a frequency dependent amplitude deviation. It exceeds 10 percent at 33 Hz. The right column in Figure 2 show the results of using a bandlimited approximation to the step function at the interface. Both amplitude and traveltime errors are negligible.

In the second example the interface is at 2500 m. In this case it is at the location of a node. The left column in Figure 3 show the results of using harmonic averaging based on relative volumetric contribution. Note that the node value at 2500 m is averaged since the interface coincides with this node position. There is in this case a large amplitude error of close to 50 percent ant 50 Hz. The traveltime error is less severe and gradually approaching 1 ms delay at 50 Hz. The right column in Figure 3 show the results of using a bandlimited approximation to the step function at the interface. Both amplitude

and traveltime errors are small for frequencies less than 40 Hz. From 40 to 50 Hz the amplitude error increases up to approximately 20 percent and in the same frequency interval there is an increased time advance of up to 2 ms. The results using the step-function are acceptable since most of the energy in the propagated waveform is below 40 Hz.

Snapshots of particle velocity from 2D simulations are shown in Figure 4. The interface is marked with a white line and is dipping with 18 degrees. The model consists of two half-spaces with the same compliance and density contrasts as for the 1D models discussed above. The top halfspace has a propagation velocity of 2000 m/s and the lower halfspace has a propagation velocity of 4000 m/s. Spatial steplengths are 10 m for both directions and the frequency content of the source is identical to the 1D cases above. The line of receiver stations is marked with the blue line. The displayed particle velocity is rotated with 18 degrees such that the vertical component of particle velocity is normal to the interface. Figure 4a show the result of using harmonic averaging based on relative volumetric contribution for the bulk modulus and arithmetic averaging of the density also based on relative volumetric contribution. The diffractions due to the staircase effect are clearly visible in Figure 4a. Figure 4b shows the results of using a bandlimited approximation to the step function at the interface. The diffractions due to the staircase effect are almost negligible in this case.

Zero offset data for coinciding source and receiver position is shown in Figure 5. The left column in Figure 5 show the results of using averaging at the interface and the right column shows the results of using a bandlimited approximation to the step function at the interface. The results using the step-function
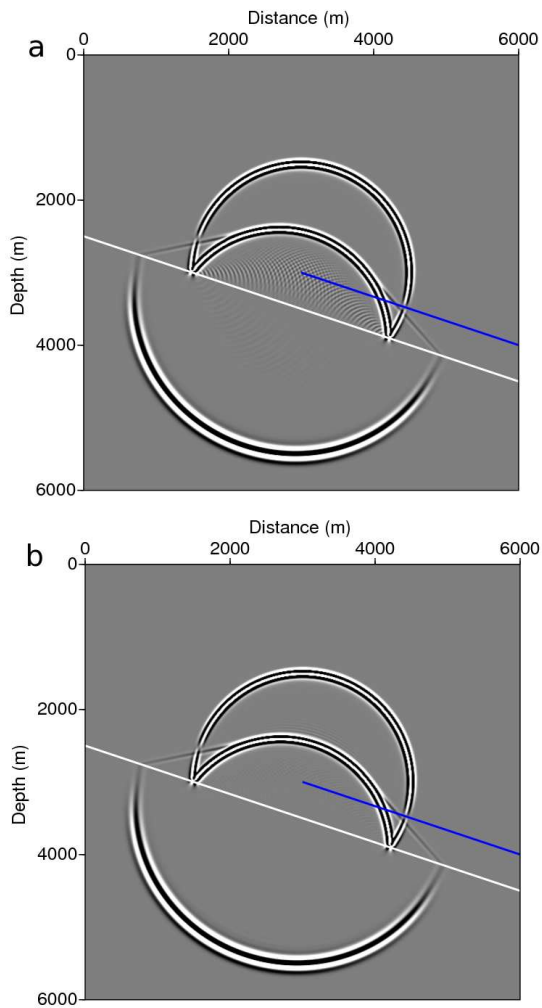
Figure 4: Vertical component of the particle velocity. The vertical component is normal to the interface marked with the white line. Receiver line in blue and source position at the start of the receiver line. a) Harmonic averaging. b) Step-function implementation.
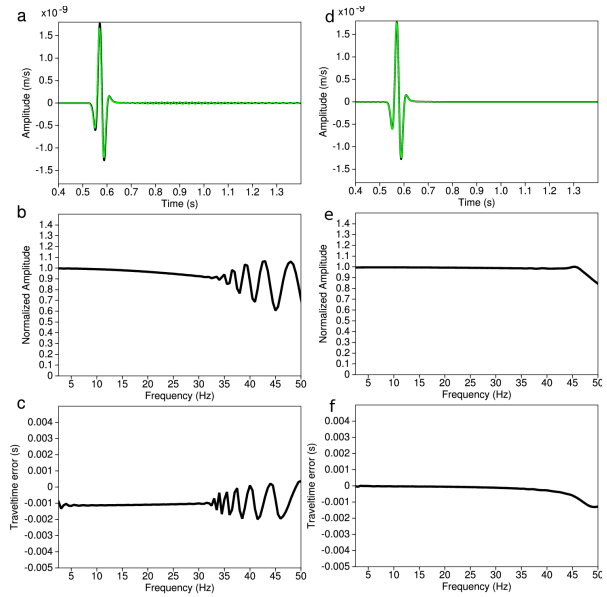

Figure 5: Left column - averaging and right column - step function. a) and d) Analytical - black and FD - green. b) and e) Amplitude ratio. c) and f) Time advance or delay.

implementation are clearly the best. The time advance in Figure 5c indicates that the effective interface position is approximately 1 m above the true interface position. The degradation in accuracy above 33 Hz is due to the staircase effect. This error contribution is predicted and explained in Mittet and Buland (1995). Also in the 2D case we see that the step-function implementation of the interface gives excellent results up to 40 Hz and then some reduction in accuracy above 40 Hz. Actually, the results for the zero offset 2D case with step-function implementation of the interface (right-hand column in Figure 5) are very similar to the corresponding 1D results for the true interface coinciding with a node location (right-hand column in Figure 3).

CONCLUSIONS

A naive implementation of an interface as a jump from one value at one node to a different value at the next node, even for the ideal case where the interface is midway between nodes, gives unacceptable modeling errors. The modeling errors can be reduced if the jump is properly bandlimited with respect to the sampling of the simulation grid.

Interfaces can be implemented at arbitrary locations in a coarse grid. Information regarding the location of an interface must be imprinted in the modeling grid. This can be done by starting from the wavenumber representation of a properly bandlimited Heaviside stepfunction and transforming it to the space domain. The source frequency must be constrained so that the spatial sampling is at 4 to 5 grid points per shortest wavelength or above, depending on the problem at hand.

REFERENCES

Anderson, J., E. V. Brytik, and G. Ayeni, 2015, Numerical temporal dispersion corrections for broadband temporal simulation, RTM and FWI: Presented at the 85th Annual International Meeting, SEG, Expanded Abstracts, 1096–1100, https://doi.org/10.1190/segam2015-5817144.1.

Dablain, M. A., 1986, The application of high-order differencing to the scalar wave equation: Geophysics, **51**, 54–66, https://doi.org/10.1190/1.1442040.

Etgen, J., 1989, Accurate wave equation modeling: SEP-60, Stanford Exploration Project, **131**, 148.

Gustafsson, B., and P. Wahlund, 2004, Time compact difference methods for wave propagation in discontinuous media: SIAM Journal on Scientific Computing, **26**, 272–293, https://doi.org/10.1137/S1064827503425900.

Mittet, R., 2017, On the internal interfaces in finite-difference schemes: Geophysics, **82**, no. 4, T159–T182, https://doi.org/10.1190/geo2016-0477.1.

Mittet, R., and A. Buland, 1995, Numerical errors due to non-aligned interfaces in coarse-grid modeling schemes: Journal of Seismic Exploration, **4**, 5–16.

Moczo, P., J. Kristek, V. Vavrycuk, R. J. Archuleta, and L. Halada, 2002, 3D heterogeneous staggered-grid finite-difference modeling of seismic motion with volume harmonic and arithmetic averaging of elastic moduli and densities: Bulletin of the Seismological Society of America, **92**, 3042–3066, https://doi.org/10.1785/0120010167.

Stork, C., 2013, Eliminating nearly all dispersion error from fd modeling and rtm with minimal cost increase: Presented at the 75th Annual International Conference and Exhibition, EAGE, Extended Abstracts, Tu 11 07, https://doi.org/10.3997/2214-4609.20130478.

Symes, W. W., and T. Vdovina, 2009, Interface error analysis for numerical wave propagation: Computational Geosciences, **13**, 363–371.

Tal-Ezer, H., 1986, Spectral methods in time for hyperbolic equations: SIAM Journal on Numerical Analysis, **23**, 11–26, https://doi.org/10.1137/0723002.

Vishnevsky, D., V. Lisitsa, V. Tcheverda, and G. Reshetova, 2014, Numerical study of the interface errors of finite-difference simulations of seismic Waves: Geophysics, **79**, no. 4, T219–T232, https://doi.org/10.1190/geo2013-0299.1.